

Patient-Derived Tumor Xenografts Are Susceptible to Formation of Human Lymphocytic Tumors¹

Gennadiy Bondarenko^{*,†,2}, Andrey Ugolkov^{*,†,2},
Stephen Rohan^{‡,§}, Piotr Kulesza^{‡,§,3},
Oleksii Dubrovskiy^{*,†}, Demirkan Gursel[§],
Jeremy Mathews[§], Thomas V. O'Halloran[†],
Jian J. Wei^{‡,§} and Andrew P. Mazar^{*,†,†}

*Center for Developmental Therapeutics, Robert H. Lurie Comprehensive Cancer Center, Northwestern University, 2170 Campus Drive, Evanston, IL, USA; †Department of Pharmacology, Feinberg School of Medicine, Northwestern University, 320 East Superior Street, Chicago, 60611, IL, USA; ‡Department of Pathology, Feinberg School of Medicine, Northwestern University, 303 East Chicago Avenue, Chicago, 60611, IL, USA; §Pathology Core Facility, Robert H. Lurie Comprehensive Cancer Center, Northwestern University, 710 North Fairbanks Court, Chicago, IL, USA; ¶Chemistry of Life Processes Institute, Northwestern University, 2170 Campus Drive, Evanston, IL, USA

Abstract

Patient-derived xenograft (PDX) tumor models have emerged as a new approach to evaluate the effects of cancer drugs on patients' personalized tumor grafts enabling to select the best treatment for the cancer patient and providing a new tool for oncology drug developers. Here, we report that human tumors engrafted in immunodeficient mice are susceptible to formation of B- and T-cell PDX tumors. We xenografted human primary and metastatic tumor samples into immunodeficient mice and found that a fraction of PDX tumors generated from patients' samples of breast, colon, pancreatic, bladder and renal cancer were histologically similar to lymphocytic neoplasms. Moreover, we found that the first passage of breast and pancreatic cancer PDX tumors after initial transplantation of the tumor pieces from the same human tumor graft could grow as a lymphocytic tumor in one mouse and as an adenocarcinoma in another mouse. Whereas subcutaneous PDX tumors resembling human adenocarcinoma histology were slow growing and non-metastatic, we found that subcutaneous PDX lymphocytic tumors were fast growing and formed large metastatic lesions in mouse lymph nodes, liver, lungs, and spleen. PDX lymphocytic tumors were comprised of B-cells which were Epstein-Barr virus positive and expressed CD45 and CD20. Because B-cells are typically present in malignant solid tumors, formation of B-cell tumor may evolve in a wide range of PDX tumor models. Although PDX tumor models show great promise in the development of personalized therapy for cancer patients, our results suggest that confidence in any given PDX tumor model requires careful screening of lymphocytic markers.

Neoplasia (2015) 17, 735–741

Address all correspondence to: Andrew P. Mazar, PhD, Department of Pharmacology, Feinberg School of Medicine, Chemistry of Life Processes Institute, Northwestern University, 2145 Sheridan Rd., Evanston, IL 60208.

E-mail: a-mazar@northwestern.edu

¹This study was supported by a generous donation from the Baskes family to the Robert H. Lurie Comprehensive Cancer Center, Northwestern University, and by Cancer Center Support grant 2 P30 CA060553-19 (A.P.M., A.U.) to the Robert H. Lurie Comprehensive Cancer Center, Northwestern University.

²These authors contributed equally to this study.

³In memoriam.

Received 14 May 2015; Revised 8 September 2015; Accepted 15 September 2015

© 2015 The Authors. Published by Elsevier Inc. on behalf of Neoplasia Press, Inc. This is an open access article under the CC BY-NC-ND license (<http://creativecommons.org/licenses/by-nc-nd/4.0/>).

<http://dx.doi.org/10.1016/j.neo.2015.09.004>

Introduction

Numerous murine models have been developed to study human cancer [1,2]. These models are used to investigate the factors involved in malignant transformation, invasion, and metastasis, as well as to examine response to therapy [1,2]. One of the most widely used models is the human tumor xenograft [1,2]. The patient-derived xenograft (PDX) tumor model approach is based on the transplantation of primary or metastatic human tumors directly into highly immunodeficient nonobese diabetic/severe combined immunodeficient gamma (NSG) mice followed by continuous propagation of the established heterotopic or orthotopic engraftment in mice [2–4]. Clinicians can evaluate the effects of cancer drugs on their patients' personalized tumor grafts, enabling them to select the best treatment for the cancer patient, and these models have evolved into a new tool for developers of oncology drugs [2–8]. However, there are some disadvantages and challenges of using mouse xenograft models. The lack of T-cell immune response in immunodeficient mice makes them vulnerable to T-cell-controlled infections, especially viral infections [9,10], as well as to formation of lymphoproliferative lesions [11,12]. Several recent studies revealed that human tumors engrafted in NSG and NOG (NOD/Shi-*scid*/IL-2R γ^{null}) mice are susceptible to Epstein-Barr virus (EBV)-associated lymphomagenesis [11,12]. More than 90% of humans are infected with the EBV, and the infection persists for life [13]. EBV, a member of the human herpesvirus family, is the major cause of infectious mononucleosis and is associated with several malignancies including nasopharyngeal carcinoma, gastric carcinoma, Hodgkin lymphoma, Burkitt lymphoma, and posttransplant lymphoma [13,14]. EBV can infect human B-cells, T-cells, NK cells, and epithelial cells [15]. Because B-cells are typically present in malignant solid tumors, formation of EBV-associated B-cell PDX tumor may evolve in a wide range of PDX tumor models.

Here, we report that 32% of PDX tumors generated from the given patient-derived tumor sample (including breast, colon, pancreatic, bladder, and renal cancer) can progress into EBV-positive and highly metastatic lymphocytic tumors. Our results suggest that human solid tumors engrafted in NSG mice are susceptible to formation of B- and T-cell PDX tumors and that thorough testing for lymphocytic markers should be performed to ensure that the appropriate PDX tumor model is used for the identification of personalized therapy for each patient.

Materials and Methods

The research protocol was approved by Northwestern University institutional review board, and all patients provided appropriate informed consent. Human tumor tissue samples were obtained from cancer patients and deidentified with six-digit numbers (Northwestern University Pathology Core Facility [PCF] number). Freshly resected human tumor samples were transplanted subcutaneously (SC) into NSG mice. Histopathological evaluation of tumor samples was performed by board-certified pathologists (S.R. and J.W.). When SC PDX tumor reached 1.5 cm in its largest dimension, the mouse was euthanized. Subcutaneous PDX tumor and mouse spleen, lymph nodes (LN), liver, and lung were collected; fixed in 10% formalin; and processed for paraffin embedding. Paraffin sections (5 μm) were stained with hematoxylin and eosin (H&E) for initial histopathological evaluation. For immunohistochemical (IHC) staining, we used antibodies against the leukocyte common antigen CD45 (monoclonal mouse anti-human, final concentration 5 $\mu\text{g}/\text{ml}$; Dako, Carpinteria, CA), B-cell specific surface protein CD20 (monoclonal mouse anti-human, final concentration 0.63 $\mu\text{g}/\text{ml}$; Dako, Carpinteria, CA), pan-T-cell specific marker CD3 (polyclonal rabbit anti-human, final concentration 6 $\mu\text{g}/\text{ml}$; Dako, Carpinteria, CA), and epithelial cell pan-cytokeratin (monoclonal mouse anti-human, final concentration 0.5 $\mu\text{g}/\text{ml}$; Thermo Scientific, Fremont, CA). IHC staining was visualized with Dako Envision+ /HRP kit according to the manufacturer's recommended procedure. *In situ* hybridization (ISH) for EBV-encoded RNA (EBER) was performed on a Ventana Medical Systems automated slide stainer using EBER probes and the Ventana ISH iVIEW Blue Detection Kit according to manufacturer's instructions.

tration 0.63 $\mu\text{g}/\text{ml}$; Dako, Carpinteria, CA), pan-T-cell specific marker CD3 (polyclonal rabbit anti-human, final concentration 6 $\mu\text{g}/\text{ml}$; Dako, Carpinteria, CA), and epithelial cell pan-cytokeratin (monoclonal mouse anti-human, final concentration 0.5 $\mu\text{g}/\text{ml}$; Thermo Scientific, Fremont, CA). IHC staining was visualized with Dako Envision+ /HRP kit according to the manufacturer's recommended procedure. *In situ* hybridization (ISH) for EBV-encoded RNA (EBER) was performed on a Ventana Medical Systems automated slide stainer using EBER probes and the Ventana ISH iVIEW Blue Detection Kit according to manufacturer's instructions.

Results

We established PDX tumors in NSG mice by SC transplantation of freshly resected tumors obtained from breast, colon, pancreatic, bladder, and renal cancer patients. At the first passage of PDX tumor, we found that a fraction of PDX tumors generated from patient samples of breast (one of three cases), colon (two of seven cases), pancreatic (one of five cases), bladder (one of two cases), and renal (one of two cases) cancer was histologically similar to lymphocytic neoplasm (Figures 1–5). We found that 15 of 22 (68%) PDX tumors (generated from patients' samples of breast, colon, pancreatic, bladder, and renal cancer) resembled histopathological characteristics of original human carcinoma, whereas 7 of 22 (32%) PDX tumors were comprised of lymphocyte-like cells. Some of SC lymphocytic PDX tumors had rare inclusions of carcinoma cells. Histologically, we found proliferation of a mixed population of mononuclear cells, ranging from small lymphocytes or plasma cells to large atypical lymphoid cells with pleomorphic nuclei and abundant basophilic cytoplasm resembling lymphoblastoid cells, in lymphocytic SC and metastatic PDX tumors (Figures 2, 4, and 5). Strikingly, whereas SC PDX tumors resembling primary human carcinoma histology were slow growing and nonmetastatic, we found that SC lymphocytic PDX tumors were fast growing and formed large metastatic lesions in mouse spleen, lymph nodes, liver, and lung (Figure 1; Table 1). To differentiate between poorly differentiated carcinoma and lymphocytic PDX tumor, we immunophenotyped lymphocytic-like PDX tumors using immunohistochemical staining for analysis of cytokeratin, CD45, CD20, and CD3 expression and ISH for detection of EBV (EBER). Because EBV does not infect rodent cells [16], EBER-positive staining was used as a marker of infected human cells in mouse tissue. Immunohistochemical staining showed that both human leukocyte common antigen CD45 and B-cell antigen CD20 were expressed in EBER-positive lymphocytic cells in 6 of 7 lymphoid PDX tumors and corresponding metastatic lesions (Figures 4 and 5; Supplementary Figures 1–3). Our findings of EBER-positive staining in lymphocytic PDX tumors suggest that EBV-associated lymphomagenesis may lead to development of human B-cell PDX tumors from xenografted human carcinomas because of the high prevalence of EBV in humans and the presence of EBV-infected B cells in solid human tumors.

In one case, we found that the first passage of breast PDX tumor (PCF #373342) grew as an EBER-positive lymphocytic neoplasm in one mouse and as a poorly differentiated adenocarcinoma in another mouse after initial subcutaneous transplantation of the same sample of metastatic pleural effusion obtained from a breast cancer patient (Table 1; Figure 3A). B-cell origin of lymphocytic PDX tumor (PCF #373342) was confirmed by IHC staining showing that lymphocytic cells were cytokeratin negative, CD45 positive, and CD20 positive (Table 1; Figure 4). The growth of the SC lymphocytic PDX tumor

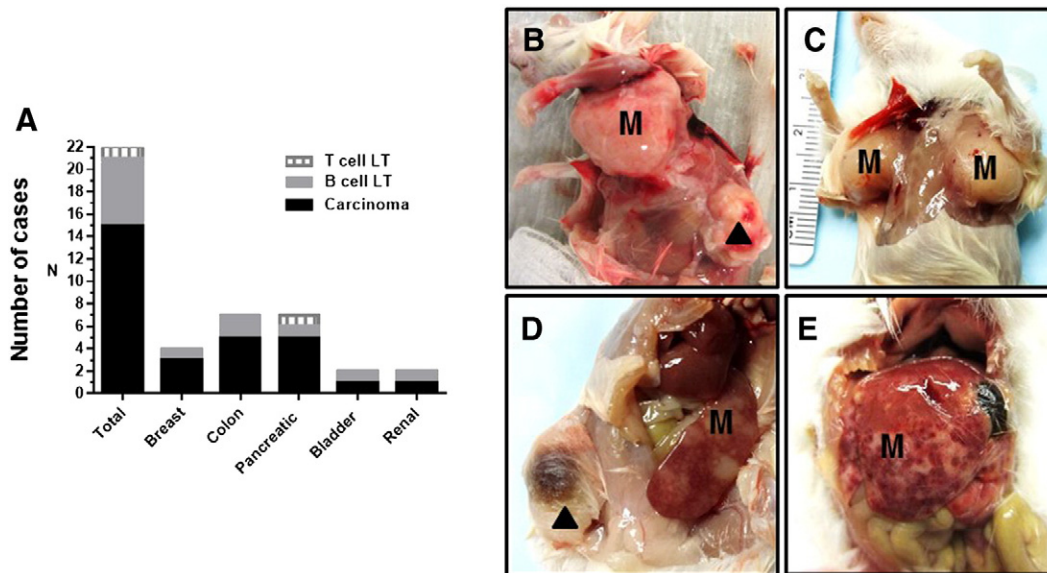


Figure 1. Histopathological characterization of established PDX tumors. (A) Twenty-two PDX tumors were generated using transplantation of human tumor samples obtained from 16 cancer patients. (B–E) Representative pictures of gross examination of NSG mice bearing lymphocytic SC PDX tumors established from bladder (B), breast (C and D), and colon (E) human tumor samples. Lymphocytic metastatic lesions were detected in mouse axillary lymph nodes (B and C), spleen (D), and liver (E). ▲, SC lymphoid PDX tumor. M, metastasis.

(PCF #373342) led to development of lymph node, lung, and liver metastases, whereas the adenocarcinoma PDX from this same patient's pleural effusion did not metastasize (Table 1; Figure 4). Further B-cell SC PDX tumor (PCF #373342) retransplantations and passages showed similar aggressive B-cell PDX tumor growth and development of distant metastasis in NSG mice. In another case, after

initial subcutaneous transplantation of a human primary pancreatic tumor (PCF #379419) into NSG mice, one mouse developed EBER-positive B-cell PDX tumor, whereas another mouse developed an EBER-negative T-cell PDX tumor (Table 1; Figures 3B and 5, A and B). T-cell origin of the lymphocytic PDX tumor (PCF #379419) was confirmed by IHC staining showing that lymphoid cells were

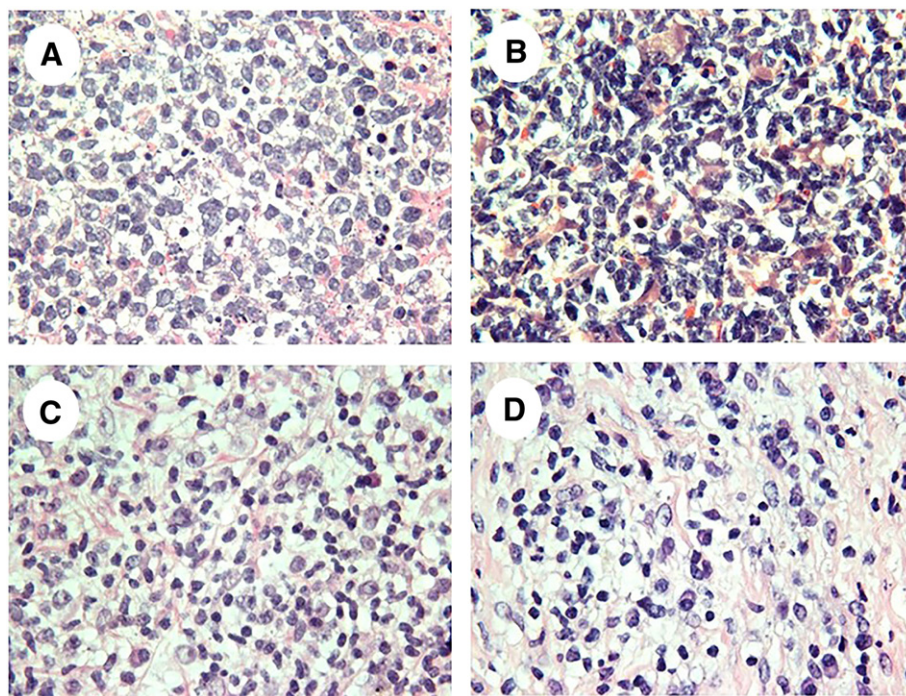


Figure 2. Lymphocytic SC PDX tumors are formed by B- or T-cells. Representative H&E images of lymphocytic SC PDX tumors established from breast (A, B-cell SC PDX tumor), bladder (B, B-cell SC PDX tumor), and pancreatic (C, T-cell SC PDX tumor; D, B-cell SC PDX tumor) human tumor samples.

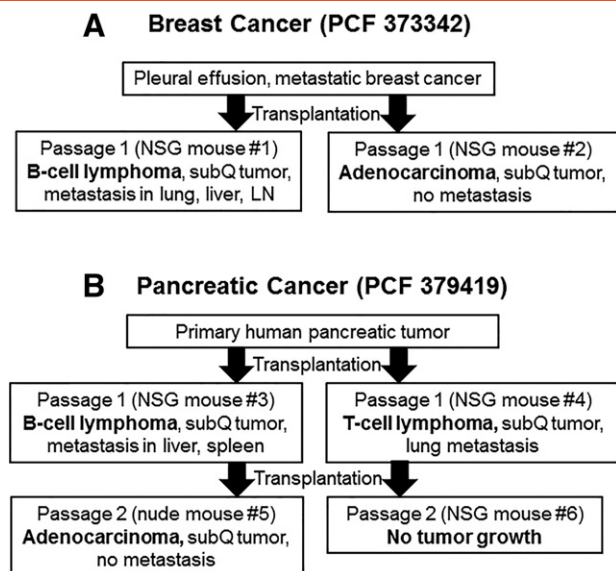


Figure 3. Development of PDX tumors of different origin (lymphocytic tumor and adenocarcinoma) from the same patient tumor sample. (A) Breast PDX tumor model. First passage of breast PDX tumor (PCF #373342) grew as lymphocytic neoplasm in one mouse and as a poorly differentiated adenocarcinoma in another mouse after the initial SC transplantation of the same sample of a metastatic pleural effusion obtained from a breast cancer patient. (B) Pancreatic PDX tumor model. After initial SC transplantation of human primary pancreatic tumor (PCF #379419) into NSG mice, one mouse developed a B-cell PDX tumor, whereas another mouse developed an SC T-cell PDX tumor. The T-cell PDX tumor did not grow after retransplantation, whereas the B-cell PDX tumor progressed to a nonmetastatic pancreatic PDX tumor (adenocarcinoma) after retransplantation.

cytokeratin negative, CD45 positive, CD20 negative, and CD3 positive (Table 1; Figure 5B). T- and B-cell PDX tumors (PCF #379419) developed distant metastases in mouse lung (T-cell), liver

(B-cell), and spleen (B-cell) (Figure 1; Table 1). Because of the small inclusions of pancreatic carcinoma cells in the B-cell SC PDX tumor (PCF #379419), further SC retransplantation of this tumor in nude mouse led to the eventual development of a pancreatic PDX tumor resembling moderately differentiated adenocarcinoma (Figure 3B). Thus, retransplantation of SC B-cell PDX tumor from NSG to nude mouse helps to clear SC PDX tumor from EBV-positive B cells leading to formation of carcinoma (Figure 3B). Furthermore, we found that PDX lymphocytic tumors did not grow in nude mice after retransplantation from NSG mice. In nude mice, we observed that PDX tumors could grow only as carcinomas. Probably, this phenomenon can be explained by the fact that nude mice maintain NK cells (participate in the immune response to EBV) which are not available in highly immunodeficient NSG mice.

We found that the morphology and immunophenotype of tumor cells in the metastatic lymphoid tumors corresponded to those found in SC lymphocytic PDX tumors: EBER positive, CD45 positive, CD20 positive and EBER negative, CD45 positive, CD20 negative, CD3 positive in B- and T-cell PDX tumors, respectively (Table 1; Figures 4 and 5). We found that EBER-positive metastatic PDX B-cells could completely replace benign cells in mouse spleen, whereas the foci of liver metastasis ranged from small periportal lesions to diffuse infiltration lesions that altered hepatic histological architecture (Figures 4 and 5; Supplementary Figures 1 and 2). We revealed that mice with small lymphocytic metastases in the liver did not show metastatic tumors in lung. Our findings also demonstrate that mouse spleen is likely the most affected organ by the dissemination of lymphoid metastatic cells from SC lymphocytic PDX tumor.

Our results suggest that PDX tumors engrafted in immunodeficient NSG mice are susceptible to formation of aggressive and metastatic lymphocytic PDX tumors and that thorough testing for lymphocytic markers should be performed to ensure that appropriate PDX tumor model is used for the identification of personalized therapy for each patient.

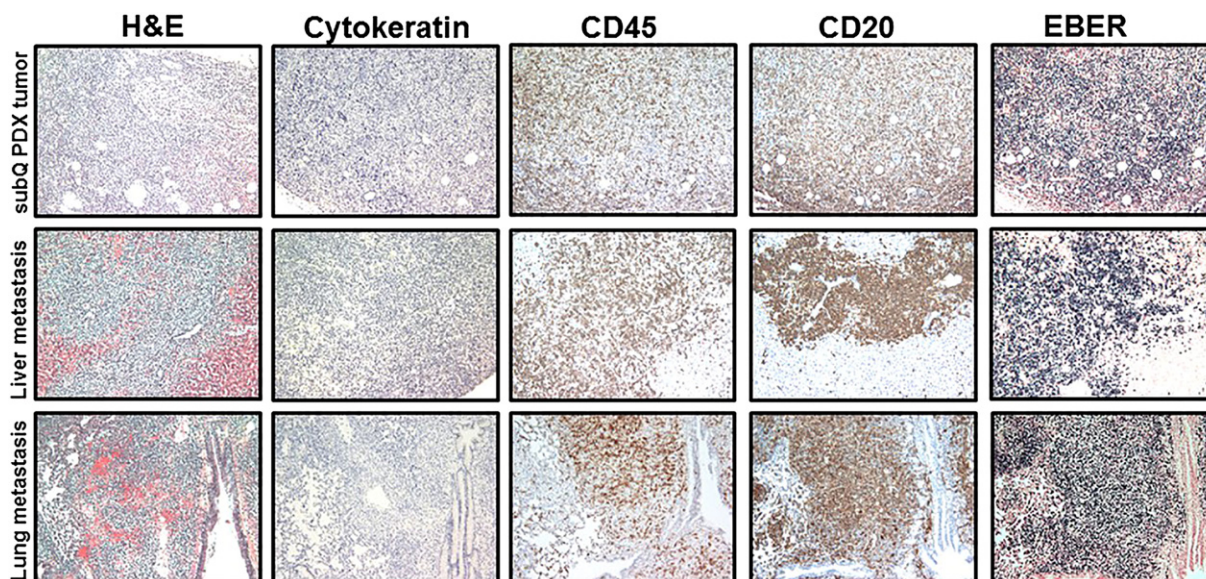


Figure 4. B-cell SC and metastatic PDX tumors established from metastatic pleural effusion obtained from a breast cancer patient (PCF #373342). Representative pictures of H&E, cytokeratin, CD45, CD20, and EBER staining in B-cell SC and metastatic PDX tumors in liver and lung. Lymphoid cells replaced original breast carcinoma cells (negative IHC staining for cytokeratin) in an SC PDX tumor. Proliferation of CD45-positive, CD20-positive (brown) leukocytes (B cell) with very strong positive EBER staining (dark blue) was observed in SC and metastatic lymphocytic PDX tumors.

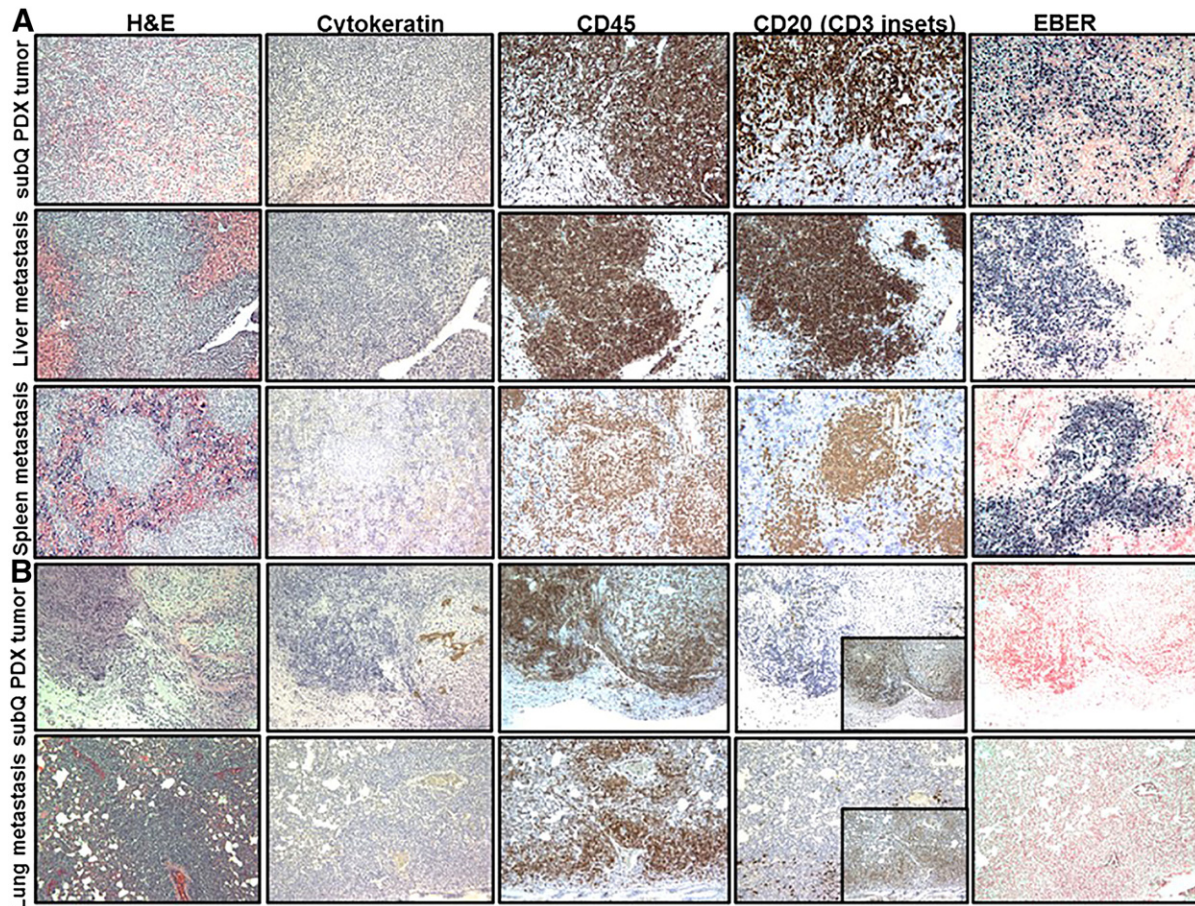


Figure 5. Lymphocytic SC and metastatic PDX tumors established from primary tumor obtained from a pancreatic cancer patient (PCF #379419). (A) Representative pictures H&E, cytokeratin, CD45, CD20, and EBER staining in B-cell SC and metastatic PDX tumors in liver and spleen. Proliferation of CD45-positive, CD20-positive (brown) leukocytes (B cell) with strong positive EBER staining (dark blue) was observed in SC and metastatic B-cell PDX tumors. (B) Representative pictures of H&E, cytokeratin, CD45, CD20, CD3, and EBER staining in T-cell SC PDX tumors and lung metastasis. Proliferation of CD45-positive, CD20-negative (with inset of CD3-positive cells) (brown), and EBER-negative leukocytes (T-cell) was observed in SC and metastatic T-cell PDX tumors.

Discussion

Although the use of immunodeficient mice contributes to better efficiency of human tumor xenotransplantation [2], establishing PDX tumor models in NSG mice has presented some challenges and limitations. The lack of an intact immune system affects tumor growth as well as metastasis [17]. The lack of T-cell immune response in immunodeficient mice makes them vulnerable to T-cell-controlled infections, especially viral infections [9,10]. It has been reported that T-cells play a prominent role in controlling EBV-associated oncogenesis [18]. Most people are infected with EBV [15]. Because EBV can infect human B-cells and T-cells which are typically present in solid malignant tumor [19], EBV-associated lymphocytic PDX tumors may develop as a result of xenotransplantation of human solid tumor to immunodeficient mice [11,12]. The potential development of lymphocytic PDX tumors instead of an expected carcinoma may significantly affect or mislead the efforts of clinicians to evaluate the effects of cancer drugs on a particular patient's tumor grafts, leading to the selection of inappropriate clinical treatments for that patient.

Our study demonstrates that PDX tumor (developed from patient samples of breast, colon, pancreatic, bladder, and renal cancer) progressed to highly metastatic lymphocytic PDX tumor in 7 of 22 (32%) cases after initial SC transplantation of human tumor samples in NSG mice. Our results are supported by a recently published study

demonstrating the development of EBV-associated B-cell PDX tumors in 11 of 21 xenografts generated in NSG mice from 16 independent patient tumor samples of hepatocellular carcinoma [12]. However, subcutaneous B-cell PDX tumors in that study were not metastatic in NSG mice [12]. Our results demonstrate that SC lymphocytic PDX tumors are fast growing and form large metastatic lesions in NSG mouse spleen, lymph nodes, liver, and lung. In contrast to SC lymphocytic PDX tumors, we found that SC PDX tumors resembling primary human carcinoma histology were slow growing and nonmetastatic. These findings suggest that metastatic lesions in lymph nodes, spleen, lung, or liver could serve as potential markers of growing lymphocytic but not carcinoma PDX tumor after initial SC transplantation of human tumor sample.

Our results show that EBV-associated lymphocytic PDX tumors may be developed in NSG mice after initial transplantation of a wide range of human carcinomas (breast, colon, pancreatic, bladder, and renal). Another recently published study has demonstrated the development of EBV-associated lymphocytic PDX tumors from colorectal, gastric, breast, and lung tumor samples transplanted SC to NOG mice [11]. In established PDX tumor models, the incidence of lymphocytic PDX tumors was 56% (19 of 33), 76% (13 of 17), 50% (2 of 4), and 67% (4 of 6) after initial transplantation of human colorectal, gastric, breast, and lung tumors in NOG mice, respectively

Table 1. Analysis of Histopathological Features of Subcutaneous and Metastatic Lymphocytic PDX Tumors

| Original Human Tumor Type | Sample ID (PCF #) | PDX Tumor | Staining | | | |
|---------------------------|-------------------|-----------|-------------|----------|----------|----------|
| | | | Cytokeratin | CD45 | CD20 | EBER |
| Breast | 373342 | SC | Negative | Positive | Positive | Positive |
| | | Liver | Negative | Positive | Positive | Positive |
| | | Lung | Negative | Positive | Positive | Positive |
| Colon | 373888 | LN | Negative | Positive | Positive | Positive |
| | | SC | Negative | Positive | Positive | Positive |
| Colon | 366786 | Liver | Negative | Positive | Positive | Positive |
| | | Spleen | Negative | Positive | Positive | Positive |
| | | LN | Negative | Positive | Positive | Positive |
| Pancreatic (CD3 negative) | 379419 | SC | Negative | Positive | Positive | Positive |
| | | Liver | Negative | Positive | Positive | Positive |
| | | Spleen | Negative | Positive | Positive | Positive |
| Pancreatic (CD3 positive) | 379419 | SC | Negative | Positive | Negative | Negative |
| | | Lung | Negative | Positive | Negative | Negative |
| Bladder | 380955 | SC | Negative | Positive | Positive | Positive |
| | | Liver | Negative | Positive | Positive | Positive |
| | | Lung | Negative | Negative | Negative | Negative |
| | | Spleen | Negative | Positive | Positive | Positive |
| | | LN | Negative | Positive | Positive | Positive |
| Renal | 366752 | SC | Negative | Positive | Positive | Positive |
| | | Liver | Negative | Positive | Positive | Positive |
| | | Lung | Negative | Positive | Positive | Positive |
| | | LN | Negative | Positive | Positive | Positive |

[11]. Histopathologically, Fujii et al. found lymphocytic metastatic lesions in mouse spleen (all mice), liver, and kidney (1 of 6 mice) obtained from six NOG mice which developed SC lymphocytic PDX tumors after initial transplantation of human colorectal tumor samples [11].

Here, we also report the development of a T-cell PDX tumor after initial transplantation of a human pancreatic carcinoma sample to NSG mice. Our findings suggest that lymphocytic PDX tumors not only are represented by EBV-associated B-cell tumors but may also originate from EBV-negative T-cells (CD45 positive, CD3 positive, CD20 negative). We found that lymphocytic PDX tumors can form hematogenous (spleen, liver, and lung) and lymphogenous (lymph node) metastases (Table 1). However, the formation of SC and metastatic T-cell PDX lesions might also reflect xenogeneic graft versus host disease. A previous study described polyclonal disease-unrelated cotransplanted donor human T-lymphocyte expansion in NSG recipient mice [20]. In one study, donor T-cells mediated xenogeneic graft versus host disease and masked the engraftment of human AML in mice [20]. Other studies demonstrated significant accumulation of donor T-cells in spleen, whereas expression of homing receptors could direct T-cells to skin [21], lung [22], and liver [23,24].

In conclusion, our results suggest that human tumors engrafted in NSG mice are susceptible to formation of lymphocytic PDX tumors and emphasize the need for thorough testing for lymphocytic markers to ensure that the appropriate (nonlymphocytic) PDX tumor model is used for the identification of personalized therapy for cancer patients.

Supplementary data to this article can be found online at <http://dx.doi.org/10.1016/j.neo.2015.09.004>.

References

[1] Richmond A and Su Y (2008). Mouse xenograft models vs GEM models for human cancer therapeutics. *Dis Model Mech* **1**, 78–82. <http://dx.doi.org/10.1242/dmm.000976>.

- [2] Siolas D and Hannon GJ (2013). Patient-derived tumor xenografts: transforming clinical samples into mouse models. *Cancer Res* **73**, 5315–5319. <http://dx.doi.org/10.1158/0008-5472.CAN-13-1069>.
- [3] Scott CL, Becker MA, Haluska P, and Samimi G (2013). Patient-derived xenograft models to improve targeted therapy in epithelial ovarian cancer treatment. *Front Oncol* **3**, 295. <http://dx.doi.org/10.3389/fonc.2013.00295>.
- [4] Hidalgo M, Amant F, Biankin AV, Budinská E, Byrne AT, Caldas C, Clarke RB, de Jong S, Jonkers J, and Mølandsmo GM, et al (2014). Patient-derived xenograft models: an emerging platform for translational cancer research. *Cancer Discov* **4**(9), 998–1013.
- [5] Rygaard J and Povlsen CO (1969). Heterotransplantation of a human malignant tumour to "nude" mice. *Acta Pathol Microbiol Scand* **77**(4), 758–760.
- [6] Hoffman RM (2010). Orthotopic mouse models expressing fluorescent proteins for cancer drug discovery. *Expert Opin Drug Discov* **5**(9), 851–866. <http://dx.doi.org/10.1517/17460441.2010.510129>.
- [7] Lindberg JM, Newhook TE, Adair SJ, Walters DM, Kim AJ, Stelow EB, Parsons JT, and Bauer TW (2014). Co-treatment with panitumumab and trastuzumab augments response to the MEK inhibitor trametinib in a patient-derived xenograft model of pancreatic cancer. *Neoplasia* **16**(7), 562–571. <http://dx.doi.org/10.1016/j.neo.2014.06.004>.
- [8] Mattie M, Christensen A, Chang MS, Yeh W, Said S, Shostak Y, Capo L, Verlinsky A, An Z, and Joseph I, et al (2013). Molecular characterization of patient-derived human pancreatic tumor xenograft models for preclinical and translational development of cancer therapeutics. *Neoplasia* **15**(10), 1138–1150.
- [9] Diebel KW, Oko LM, Medina EM, Niemeyer BF, Warren CJ, Claypool DJ, Tibbetts SA, Cool CD, Clambey ET, and van Dyk LF (2015). Gammaherpesvirus small noncoding RNAs are bifunctional elements that regulate infection and contribute to virulence in vivo. *MBio* **6**, e01670-14. <http://dx.doi.org/10.1128/mBio.01670-14>.
- [10] Hillen KM, Gather R, Enders A, Pircher H, Aichele P, Fisch P, Blumenthal B, Schamel WW, Straub T, and Goodnow CC, et al (2015). T cell expansion is the limiting factor of virus control in mice with attenuated TCR signaling: implications for human immunodeficiency. *J Immunol* **194**, 2725–2734. <http://dx.doi.org/10.4049/jimmunol.1400328>.
- [11] Fujii E, Kato A, Chen YJ, Matsubara K, Ohnishi Y, and Suzuki M (2014). Characterization of EBV-related lymphoproliferative lesions arising in donor lymphocytes of transplanted human tumor tissues in the NOG mouse. *Exp Anim* **63**, 289–296.
- [12] Chen K, Ahmed S, Adeyi O, Dick JE, and Ghanekar A (2012). Human solid tumor xenografts in immunodeficient mice are vulnerable to lymphomagenesis associated with Epstein-Barr virus. *PLoS One* **7**, e39294. <http://dx.doi.org/10.1371/journal.pone.0039294>.
- [13] Carbone A, Gloghini A, and Doti G (2008). EBV-associated lymphoproliferative disorders: classification and treatment. *Oncologist* **13**, 577–585. <http://dx.doi.org/10.1634/theoncologist.2008-0036>.
- [14] Cohen JI, Mocarski ES, Raab-Traub N, Corey L, and Nabel GJ (2013). The need and challenges for development of an Epstein-Barr virus vaccine. *Vaccine* **31**(Suppl. 2), B194–96. <http://dx.doi.org/10.1016/j.vaccine.2012.09.041>.
- [15] Cohen JI, Kimura H, Nakamura S, Ko YH, and Jaffe ES (2009). Epstein-Barr virus-associated lymphoproliferative disease in non-immunocompromised hosts: a status report and summary of an international meeting, 8–9 September 2008. *Ann Oncol* **20**, 1472–1482. <http://dx.doi.org/10.1093/annonc/mdp064>.
- [16] Ma SD, Hegde S, Young KH, Sullivan R, Rajesh D, Zhou Y, Jankowska-Gan E, Burlingham WJ, Sun X, and Gulley ML, et al (2011). A new model of Epstein-Barr virus infection reveals an important role for early lytic viral protein expression in the development of lymphomas. *J Virol* **85**(1), 165–177. <http://dx.doi.org/10.1128/JVI.01512-10>.
- [17] Kobayashi T, Owczarek TB, McKiernan JM, and Abate-Shen C (2015). Modelling bladder cancer in mice: opportunities and challenges. *Nat Rev Cancer* **15**, 42–54. <http://dx.doi.org/10.1038/nrc3858>.
- [18] Thorley-Lawson DA and Gross A (2004). Persistence of the Epstein-Barr virus and the origins of associated lymphomas. *N Engl J Med* **350**, 1328–1337.
- [19] Stockmann C, Schadendorf D, Klose R, and Helfrich I (2014). The impact of the immune system on tumor: angiogenesis and vascular remodeling. *Front Oncol* **4**, 69. <http://dx.doi.org/10.3389/fonc.2014.00069>. eCollection 2014.
- [20] von Bonin M, Wermke M, Cosgun KN, Thiede C, Bornhauser M, and Wagemaker G, et al (2013). In vivo expansion of co-transplanted T cells impacts on tumor re-initiating activity of human acute myeloid leukemia in NSG mice. *PLoS One* **8**, e60680. <http://dx.doi.org/10.1371/journal.pone.0060680>.

- [21] Ali N, Flutter B, Sanchez Rodriguez R, Sharif-Paghaleh E, Barber LD, Lombardi G, and Nestle FO (2012). Xenogeneic graft-versus-host-disease in NOD-scid IL-2R γ null mice display a T-effector memory phenotype. *PLoS One* **7**, e44219. <http://dx.doi.org/10.1371/journal.pone.0044219>.
- [22] Covassin L, Laning J, Abdi R, Langevin DL, Phillips NE, Shultz LD, and Brehm MA (2011). Human peripheral blood CD4 T cell-engrafted non-obese diabetic-scid IL2r γ (null) H2-Ab1 (tm1Gru) Tg (human leucocyte antigen D-related 4) mice: a mouse model of human allogeneic graft-versus-host disease. *Clin Exp Immunol* **166**, 269–280. <http://dx.doi.org/10.1111/j.1365-2249.2011.04462.x>.
- [23] Gregoire-Gauthier J, Durrieu L, Duval A, Fontaine F, Dieng MM, Bourgey M, Patey-Mariaud de Serre N, Louis I, and Haddad E (2012). Use of immunoglobulins in the prevention of GvHD in a xenogeneic NOD/SCID/ γ c-mouse model. *Bone Marrow Transplant* **47**, 439–450. <http://dx.doi.org/10.1038/bmt.2011.93>.
- [24] Laing ST, Griffey SM, Moreno ME, and Stoddart CA (2015). CD8-positive lymphocytes in graft-versus-host disease of humanized NOD.Cg-Prkdc (scid)Il2rg(tm1Wj)/SzJ mice. *J Comp Pathol* **152**, 238–242. <http://dx.doi.org/10.1016/j.jcpa.2014.12.010>.